Macromolecules

Article

pubs.acs.org/Macromolecules

Mechanoluminescent Imaging of Osmotic Stress-Induced Damage in a Glassy Polymer Network

Jess M. Clough,[†] Jasper van der Gucht,[‡] and Rint P. Sijbesma*[,†]

[†]Laboratory of Macromolecular and Organic Chemistry and the Institute for Complex Molecular Systems, Eindhoven University of Technology, P.O. Box 513, 5600 MB, Eindhoven, The Netherlands

[‡]Laboratory of Physical Chemistry and Soft Matter, Agrotechnology and Food Sciences Group, Wageningen University, PO Box 8038, 6700 EK Wageningen, The Netherlands

Supporting Information

ABSTRACT: A chemiluminescent mechanophore, bis(adamantyl-1,2-dioxetane), is used to investigate the covalent bond scission resulting from the sorption of chloroform by glassy poly(methyl methacrylate) (PMMA) networks. Bis(adamantyl)-1,2-dioxetane units incorporated as cross-linkers underwent mechanoluminescent scission, demonstrating that solvent ingress caused covalent bond scission. At higher cross-linking densities, the light emission took the form of hundreds of discrete bursts, widely varying in intensity, with each burst composed of 10^7−10^9 photons. Camera imaging indicated a relatively slow propagation of bursts through the material and permitted analysis of the spatial correlation between the discrete bond-breaking events. The implications of these observations for the mechanism of sorption and fracture are discussed.

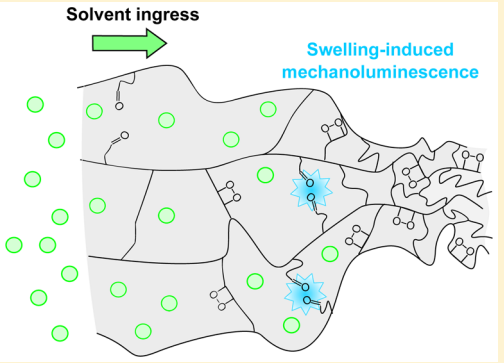

INTRODUCTION

Many polymers are exposed to solvent in their end-use applications, for example, in sealants,[1] coatings,[2] membranes,[3−5] controlled release systems, especially for pharmaceuticals[6,7] and tissue engineering,[6,8,9] or to generate complex architectures, as in microlithography.[10−12] The sorption of solute by polymeric materials encompasses a broad range of physical phenomena, such as dissolution, diffusion, swelling, and relaxation, with concomitant stress buildup and deformation or even failure of the polymeric matrix.[13−15] In particular, glassy polymers provide not only entropic resistance to swelling, as described in Flory−Rehner theory, but also additional viscous resistance from limited chain mobility.[16−18] In these materials, solvent uptake is controlled by polymer relaxation processes, giving rise to a sharp diffusion front and a linear relationship between solvent uptake and time. Such behavior is characteristic of Case II sorption. The resulting osmotic stresses in these systems have been predicted to be of the order of 10 MPa or greater:[19,20] the growing swollen part of the polymer matrix exerts tensile stresses on the unswollen polymer that can even lead to fracture. However, while much experimental and theoretical study has been devoted to understanding the physical processes involved in the swelling of polymeric materials, particularly the sharp solvent front in glassy polymers,[21−28] little is known about the forces experienced by the polymer chains at the molecular level. A better description of the mechanical effects at these length scales would permit finer control over polymeric responses to solvent ingress, for example, to tune the release time of a drug from a polymeric carrier, to create nanostructures in membranes with greater accuracy, or to mimic the mechanical response of natural structural tissues.[29]

In the past 10 years, new approaches to visualizing molecular stress distributions in polymeric materials have emerged from the field of polymer mechanochemistry. By directing the large forces that accumulate along polymer chains, chemists in this area have designed materials that give productive mechanical responses, such as reporting or repairing damage that the materials have themselves sustained. To obtain these properties, functional groups with relatively weak covalent bonds, or mechanophores, are incorporated in the material, which isomerize or break selectively when a force is applied.[30−36] Mechanoresponsivity is thereby achieved without significantly compromising the mechanical integrity of the material.

The mechanical response of polymeric systems to solvent sorption has received some prior attention in this line of research. The first studies found no evidence of mechanical activation of covalent mechanophores: neither scission of disulfide bonds[37] nor Bergman cyclization of ene−diynes[38] were found to occur in swelling polymer networks cross-linked with these mechanophores. The first swelling-induced mechanoresponse was recorded by the Moore group, from bulk poly(methyl methacrylate) (PMMA) samples incorporating the mechanofluorochromic spiropyran, which undergoes an electrocyclic ring-opening to produce the strongly colored and fluorescent merocyanine under the influence of mechanical

Received: November 28, 2016
Revised: February 13, 2017
Published: March 2, 2017

DOI: 10.1021/acs.macromol.6b02540
Macromolecules 2017, 50, 2043−2053

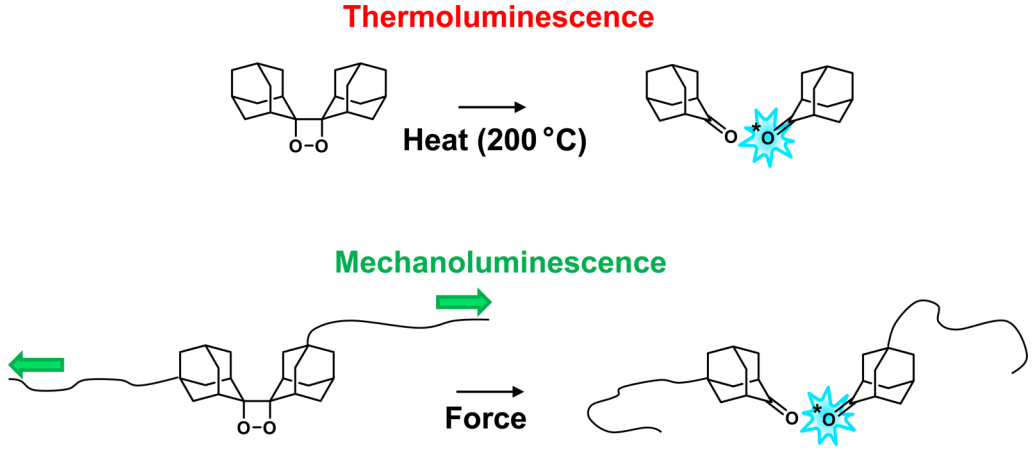

Figure 1. Top: thermally induced mechanoluminescence from bis(adamantyl)-1,2-dioxetane, first discovered by Wieringa et al.[46] At 200 °C, bis(adamantyl)-1,2-dioxetane has a half-life of approximately 100 s.[47] Bottom: on incorporating in a polymer, chemiluminescence from bis(adamantyl)-1,2-dioxetane can be induced mechanically, as first reported by Chen et al.[31]

force.[39] In this study, Lee et al. found that the fluorescence intensity of the spiropyran-functionalized PMMA correlated strongly with the swelling degree of the sample. Most recently, swelling polyelectrolytes tethered to a surface via a Diels–Alder adduct induced its retro-cycloaddition, with the resulting polymer detachment followed in situ by quartz crystal microbalance (QCM) measurements.[40] However, these approaches have significant drawbacks in monitoring and mapping the stresses brought about by solvent–polymer interactions. In particular, mechanoactivation of spiropyran gives an integrated signal in absorption or fluorescence, making it more difficult to record small changes over time. In addition, the equilibrium between spiropyran and merocyanine is sensitive to the polarity of the environment, which can be influenced by the presence of solvent. QCM meanwhile provides no spatial information.

The 1,2-dioxetane mechanophore is a highly sensitive force probe for polymeric materials which could overcome these limitations to provide a more detailed picture of swelling-induced reactivity. When incorporated covalently within a polymeric material, the four-membered dioxetane ring cleaves preferentially upon application of stress to the polymer to give ketones in their excited state, which may then relax to the ground state with the emission of mechanically induced chemiluminescence or mechanoluminescence (Figure 1).[31,41] As with other "stress reporters", dioxetane luminescence reports where a critical force for decomposition has been exceeded. This mechanophore has been used to track stress distributions in a diverse selection of polymeric materials in the solid state, such as linear polymers and acrylate networks,[31] thermoplastic elastomers,[42] multiple interpenetrating networks,[43] supramolecularly cross-linked networks,[44] and filled elastomers.[45] Mechanoluminescence offers an important advantage over techniques based on fluorescent mechanophores, namely that the signal is transient rather than additive, permitting greater spatial and temporal resolution of covalent bond-breaking events. The absence of an excitation signal, which is required to visualize the damage with mechanically induced fluorescence, further boosts the sensitivity of systems based on mechanically induced chemiluminescence.

In this study, we incorporate bis(adamantyl)-1,2-dioxetane as a cross-linker in PMMA and study the covalent bond scission processes upon solvent ingress by monitoring the mechanoluminescence with either a photodiode or a sensitive camera. We also investigate the physical mechanisms leading to solvent swelling-induced covalent bond-breaking and macroscopic fracture by systematically varying the cross-linking density and examining the distributions of bond-breaking events in magnitude and time.

EXPERIMENTAL DETAILS

Materials. Unless otherwise stated, all starting materials were obtained from commercial suppliers and used without purification. AIBN was precipitated from methanol and dried under vacuum. Methyl methacrylate monomer and diacrylate cross-linkers were filtered through a plug of basic alumina to remove the inhibitors. Dioxetane bis(acrylate) cross-linker was synthesized as previously reported.[31] Bis(adamantyl)-1,2-dioxetane was also prepared following a literature procedure.[48] All polymerization reactions were performed under a nitrogen atmosphere. Thin layer chromatography (TLC) was conducted on silica gel 60 F254 (Merck, 0.2 mm). Column chromatography was carried out on silica gel, basic alumina, or neutral alumina (0.063–0.2 mm). NMR spectra were recorded on a 400 MHz (100 MHz for ^{13}C) Varian Mercury VX spectrometer at room temperature using residual protonated solvent signals as internal standards (^{1}H: $\delta(CDCl_3)$ = 7.26 ppm; ^{13}C: $\delta(CDCl_3)$ = 77.16 ppm).

Film Preparation. In a typical experiment AIBN (40 mg, 0.244 mmol, 0.0261 equiv), dioxetane cross-linker (12.4 mg, 0.0234 mmol, 0.0025 equiv), diphenylanthracene (10 mg, 0.0302 mmol, 0.00323 equiv), tetra(ethylene glycol) diacrylate (TEGDA) (e.g., 19.1 μL, 0.00701 mmol, 0.0075 equiv for 1%; 121 μL, 0.444 mmol, 0.0475 equiv for 5%), and methyl methacrylate (MMA) (1 mL, 9.35 mmol, 1 equiv) were combined in a vial closed with a septum and flushed with argon for 3–4 min. Once dissolved, the reaction mixture was transferred to an unsealed Teflon mold, 2 cm × 4.5 cm × 5 mm, in an oven under a nitrogen atmosphere and allowed to flush with nitrogen for several minutes, after which a glass plate was placed on top of the mold. The reaction mixture was then heated for 6 h at 65 °C. The resulting films were clear, with a slight yellow color from the cross-linker, and they had a slight blue fluorescence under ambient light from the DPA.

Gravimetry Experiments. Small pieces (5 mm × 5 mm × 0.5 mm) were carefully cut from the films and placed in a small glass vial. Chloroform was added and the vial closed with a cap. After various time intervals, the sample was carefully taken out of the solvent with tweezers, solvent from its surface dried lightly with a tissue and placed in preweighed vial, and the vial closed with a lid. The weight of the sample was then recorded. The sample was placed back in the solvent, and the timing of the swelling was resumed. The samples became fragile with increasing solvent uptake: at higher cross-linking densities

DOI: 10.1021/acs.macromol.6b02540
Macromolecules 2017, 50, 2043–2053

(>4 mol %), the samples fractured in a few macroscopic pieces, after which the gravimetric experiment was not continued; at lower cross-linking densities, macroscopic fracture did not occur, but the pressure applied with the tweezers sometimes led to small pieces fracturing off from the side of the sample, leading to a slight apparent decrease in weight at longer swelling times.

Solvent Swelling Tests with Photodetector. Small pieces (5 mm × 5 mm × 0.5 mm) were carefully cut from the films and placed in a small glass vial. The photodiode measurements were conducted with a Hamamatsu S2281-01 photodiode, photoactive area 100 mm^2, spectral response given below. In these experiments, the glass vial was fixed directly on top of the photodiode with tape and covered with aluminum foil to exclude light. Solvent was injected via plastic tubing from a syringe (Figure 2). The photocurrent was recorded using an Agilent semiconductor parameter analyzer (4155 series). Read-out rates are reported with individual experiments.

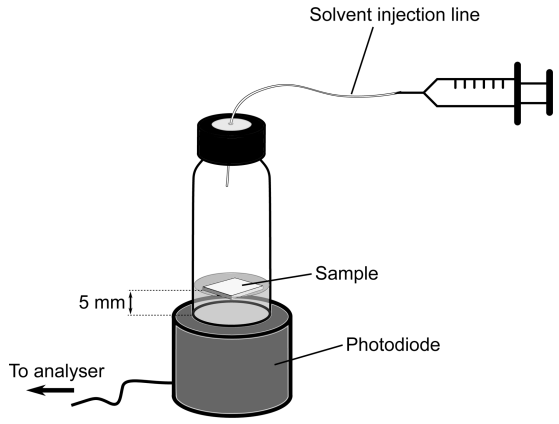

Figure 2. Schematic showing photodetection setup with photodiode.

The imaging experiments were performed with an Andor iXon Ultra 888 camera containing an EM-CCD sensor and fitted with a Micro Nikkor 40 mm *f*/2.8 macro lens that was fixed manually in its largest aperture (minimum focusing distance 0.185 m). The EM gain was set to 1000. Frame transfer and cropped sensor modes were used to increase frame rates. The frame rate settings are reported with individual experiments. For the intensity analysis, the glass vial was clamped 10 cm above the top of the lens of the camera so that the sample vial with a diameter of 1 cm occupied an area of 512 × 512 pixels in the final images. Solvent was injected; light from the environment was then excluded. A recording run of 20 000 frames was started after 5−10 min of swelling (depending on the cross-linking density), at the start of the period in which the greatest activity was observed, using the photodiode measurements as a guide to the timing of the events.

To examine spatial localization and fracture propagation, the sample was fixated in a homemade cell consisting of a wire ring and cotton string wound around the ring to make two layered webs. The sample was placed in between the two layers, and the experiment was conducted as described above. The fixation was checked before and after recording mechanoluminescence.

RESULTS

PMMA exhibits a strong response to swelling in some organic solvents, in common with other glassy polymers. To examine the swelling properties of the dioxetane-functionalized PMMA networks (for preparation details, see Experimental Details section), flat, square samples (5 mm × 5 mm × 0.5 mm) were allowed to swell in a selection of solvents for approximately 1 h, with brief intervals during which the samples were removed from the solvent to be weighed. The increase in swelling ratio with time in different solvents measured in this way is plotted in Figure 3 for a sample cross-linked with 1 mol % of tetra(ethylene glycol) diacrylate; we note that the swelling

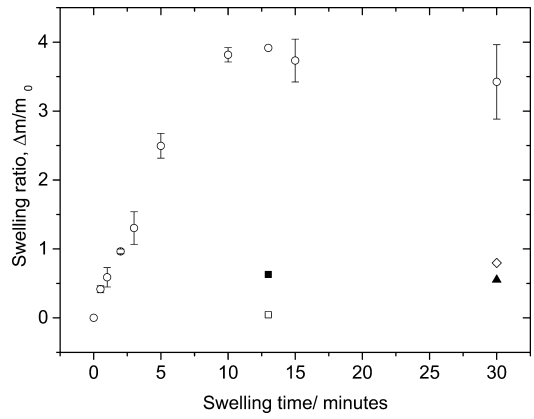

Figure 3. Swelling ratios of cross-linked poly(methyl methacrylate) films (5 mm × 5 mm × 0.5 mm), cross-linking density 1 mol % with cross-linker tetra(ethylene glycol) diacrylate), over time upon penetration of chloroform (open circle); acetonitrile (filled square); acetone (open diamond); tetrahydrofuran (filled triangle); toluene (open square). Standard deviations from three or four separate experiments.

uptake of samples containing 0.25 mol % dioxetane cross-linker and 0.75 mol % tetra(ethylene glycol) diacrylate was indistinguishable from the swelling uptake curve shown in Figure 3. Polar protic and apolar solvents, such as water and toluene, respectively, gave little measurable swelling. In polar aprotic solvents, such as acetone, ethyl acetate, acetonitrile, and tetrahydrofuran (THF), the samples took up approximately half their weight in solvent after half an hour. Chloroform swelled the samples to the greatest extent (even after accounting for the higher molar mass of the solvent) and also at the greatest rate, with the sample taking up almost 4 times its weight in solvent after approximately 10 min. On this basis, most of the experiments reported here were conducted in chloroform. Samples of the same size with 20 mol % cross-links took up less than half their weight in solvent after 5 min before becoming too fragile to weigh. In contrast to the report of Lee et al.,[39] imbibing chloroform did not cause our 1 mol % samples to fracture macroscopically, although samples with higher cross-linking densities (>4 mol %) exhibited damage on the macroscopic level: these samples were whitened after drying, possibly from crazing, and many fractured into a few macroscopic pieces (for photographs of the samples at different stages of swelling, see Supporting Information). This difference is possibly related to either the larger size of the samples in the study of Lee et al. (27.5 × 8 × 0.75 mm), or the differing swelling geometry, both of which strongly influence the swelling degree and kinetics.

Having established which solvents elicit the greatest osmotic response from PMMA, we took a sample (dimensions as described above, 5 mm × 5 mm × 0.5 mm) with a total cross-linking density of 5 mol %, dioxetane concentration 0.75 mol %, and 0.32 mol % 9,10-diphenylanthracene (DPA). DPA was added to boost the overall quantum yield, as described in prior literature.[31,41,45] Injecting chloroform onto the sample in a vial in a darkened room led to mechanoluminescence visible to the naked eye. "Firework"-like flashes of light could be observed over several minutes, following an initial induction time of approximately 4 min and ceasing entirely after 10 min.

DOI: 10.1021/acs.macromol.6b02540
Macromolecules 2017, 50, 2043−2053

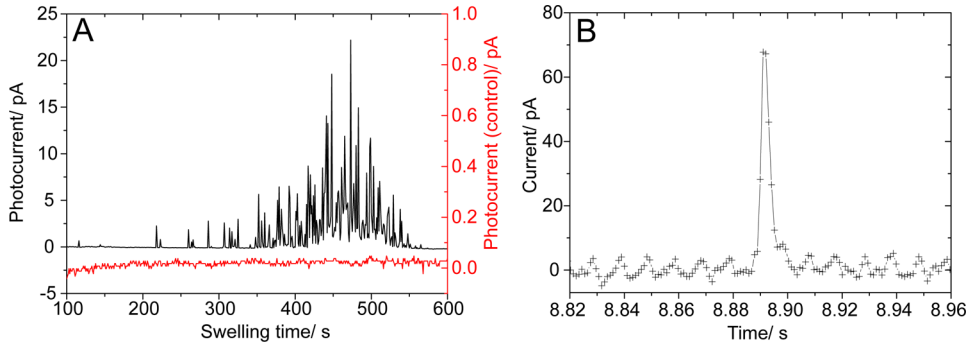

Figure 4. (A) Photocurrent recorded on swelling PMMA (0.75 mol % dioxetane cross-linker, 5 mol % total cross-linking density, 0.32 mol % DPA) with chloroform vs time from injection of solvent (black line); swelling of control sample containing molecularly dissolved dioxetane and DPA (red line). Sampling rate 1 Hz; each peak corresponds to one point at this sampling rate. (B) Photocurrent from one burst, or event, recorded at a sampling rate of 1000 Hz, each point corresponding to intensity measured during a 1 ms interval. The oscillations in the baseline result from electrical interference.

To quantify the intensity of the light emission, we performed the swelling tests on top of a photodiode as a photodetector (see Experimental Details section). Although the photodiode provided only a total intensity read-out, it allowed us to efficiently assess the effect of network characteristics on the solvent-induced mechanoluminescence. An example of the photocurrent signal that we obtained in this setup is shown in Figure 4A. The photodiode measurements confirmed the observations made by eye regarding the nature of the emission, namely, that it is composed of discrete, intermittent bursts of light, which we will also refer to as "events". The length of time during which light emission occurs also corresponded well to the time taken by the sample to reach its maximum swelling ratio, as determined from the gravimetric tests described above. Otherwise, the events appear to occur at random time intervals and with random intensities, within a range of 1−2 orders of magnitude. On drying and reswelling the samples, no further significant light emission was observed. Control photodiode measurements with a PMMA network containing molecularly dissolved bis(adamantyl)-1,2-dioxetane and 9,10-diphenylanthracene gave out no measurable light emission, demonstrating that the observed activation from covalently incorporated dioxetanes is genuinely mechanical in nature. Any heat from bond formation following covalent bond scission or released mechanical potential energy is therefore insufficient to induce dioxetane scission.

At higher read-out rates, it was possible to resolve individual bursts temporally with the photodiode (Figure 4B). We were able to determine that the length of the individual bursts was of the order of a few milliseconds, by measuring with a sampling rate of 1000 Hz. The time scale of the emission does not arise from the relaxation of the excited states: the mechanochemically generated adamantanone transfers its excitation energy via Förster resonance energy transfer (FRET) to 9,10-diphenylanthracene acceptors that are incorporated in the network, which relax from their first singlet excited (S_1) state with a lifetime of 7.6 ns in cyclohexane[49] (even in the absence of FRET, the S_1 state of adamantanone has a lifetime of approximately 9 ns[50]). The time scale of the bursts, or events, must therefore be a consequence of the bond-breaking processes. Furthermore, on the basis of the photodiode specifications (see Supporting Information), the largest of the bursts was estimated to emit in the order of 7.3×10^8 photons. Camera imaging indicated that the smallest events distinguishable from the noise were at most 2 orders of magnitude smaller than the largest events. Given that the efficiency of the mechanical production of singlet state excited states is 0.9%[41] and the efficiency of singlet−singlet energy transfer is approximately 80%, based on a previously reported R_0 value of 2.3 nm (for excited state acetone to DPA in a polystyrene film; for further information on the calculation of FRET efficiency, see Supporting Information),[51] the largest events recorded corresponded to the breaking of 1.0×10^{11} dioxetane moieties. The total light emitted in the run shown in Figure 3a corresponded to the scission of 2.4×10^{12} dioxetane moieties, or equivalently 1 out of 4.8×10^5 dioxetane groups incorporated in the sample. These figures also take into account the light-capture efficiency of the photodiode, which was calculated as 32% of the mechanoluminescence emitted from the size of the photoactive area, and the sample-to-sensor distance (for estimation of detection efficiency of photodiode setup, see Supporting Information).

The effect of cross-linking density in the PMMA network was then studied by varying the amount of a nonfunctional cross-linker, which contains a tetra(ethylene glycol) spacer, while keeping the amount of dioxetane cross-linker constant (Figure 5). A sharp transition in the amount of mechanoluminescence and number of bursts, or events, was observed on increasing the cross-linking density. At lower cross-linking densities (1 and 0.5 mol %), events occurred infrequently and at irregular intervals. At 4−5 mol % cross-linking density, far more mechanoluminescence was emitted and a strong temporal clustering of events was evident. Increasing cross-link density above this threshold led to an increase in the total amount of light emitted and an increase in the number of events. An increase in the length of induction time was also observed, which may be related to both the lower swelling rate at higher cross-linking densities and to the incorporation of a significant amount of tetra(ethylene glycol), which would be expected to lower the glass transition temperature of the network. Incorporating cross-linkers with an octa(ethylene glycol) spacer gave even longer onset times before significant mechanoluminescence could be observed, which would also provide support for the influence of glass transition temperature on the onset time (see Supporting Information). Tripling the % dioxetane cross-linker incorporated while keeping the total cross-linking density constant led to an approximate tripling of the intensities of the events (see Supporting Information).

Swelling PMMA with the other polar aprotic solvents listed in Figure 3 gave little or no mechanoluminescence, comparable

DOI: 10.1021/acs.macromol.6b02540
Macromolecules 2017, 50, 2043−2053

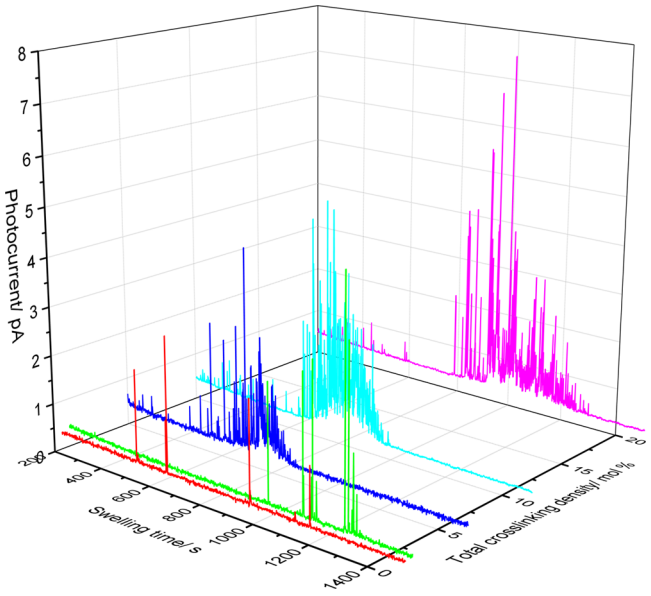

Figure 5. Effect of variation in cross-linking density of PMMA on solvent-induced mechanoluminescence. Swelling with chloroform; 1 Hz photodiode read-out rate; 0.25 mol % dioxetane cross-linker incorporation (tetra(ethylene glycol) inactive cross-linker). Total cross-linking densities: 0.5 mol % (red); 1 mol % (green); 5 mol % (dark blue); 10 mol % (light blue); 20 mol % (pink).

with the sporadic emission seen at low cross-linking densities in chloroform, even at high cross-linking densities. The swelling in these solvents was therefore not studied any further. Interestingly, swelling dioxetane cross-linked networks of poly(ethyl methacrylate) and poly(hexyl methacrylate) gave no measurable light emission with any of the solvents studied. These materials have glass transition temperatures (T_g) of 66 and −5 °C, respectively, in comparison with the T_g of PMMA, 125 °C.[52] Even after equilibration with a swelling solvent, swollen PMMA can remain glassy at 20 °C.[53,54] Glassiness appears to be a requirement for mechanoluminescence (and, by extension, covalent bond scission) upon solvent uptake. Furthermore, a sample of high molecular weight linear PMMA (M_w ∼ 100 kDa), containing a single dioxetane group close to the midpoint of each polymer chain, also gave no light on swelling on chloroform, the solvent which elicited the greatest response from cross-linked PMMA. Possibly, the molecular entanglements present at this molecular weight are insufficiently restrictive of mobility to give rise to covalent bond scission.

Imaging the solvent-induced mechanoluminescence with a sensitive camera, containing a charge-coupled device sensor connected to an electron-multiplying register (EMCCD), gave information on the locations of the covalent bond scission events, along with enhanced photosensitivity and temporal resolution. The light from swelling samples was imaged in a very similar geometry to the photodiode measurements: facing the slab-shaped sample in the direction of its greatest cross-sectional area, from the bottom of the vial (see Supporting Information). A macro lens with a short focusing distance was used to ensure good spatial resolution and to capture the most amount of light. Examples of the fracture events that could be imaged with the camera are shown in Figure 6: a broad range of event sizes and intensities were observed. MATLAB was used to quantify the event intensities from the movie frames (for a description of the script, see Supporting Information).

We used this more sensitive technique first to try to discern any underlying statistical patterns in the occurrence of solvent-induced mechanoluminescence events of particular sizes and intensities at higher cross-linking densities (>4 mol %). It was qualitatively evident from the photodiode measurements on these samples that the intensities of the individual events could not be characterized by a normal distribution: there are a small number of large events and many more smaller events, which appear to merge to give a broad hump in intensity. Recording at higher frame rates (70 Hz) with the camera permitted resolution of these smaller events. The distribution of the intensities of events spanned approximately 2 orders of magnitude, limited at low intensities by experimental noise (Figure 7). At intermediate intensities, the distribution approximately follows a power law, although it should be noted that the range of this power law extends only over roughly 1 decade in intensities. Linear regression analysis on a plot of cumulative probability vs intensity gave an exponent of 0.83 for the middle section of the curve, marked by the thick black lines in Figure 7 (20 mol %: 0.70 ± 0.08; 10 mol %: 0.90 ± 0.06; 4 mol %: 0.89 ± 0.08). There was a lower intensity cutoff to the apparent power law regime, corresponding to ∼2 × 10^4 counts in the camera's intensity units, which corresponds to approximately 112 photons *received* on the sensor (see Supporting Information for conversion factor). There was also an upper intensity cutoff at ∼3 × 10^5 counts. Events with intensities in the region of this cutoff were found to give areas in the camera images of 0.3 mm^2. We assume that the thickness of the sample (0.5 mm) imposes an upper limit on the size of that a rupture event can have. Lastly, the cross-linker content does not appear to have a significant influence on the shape of the distribution.

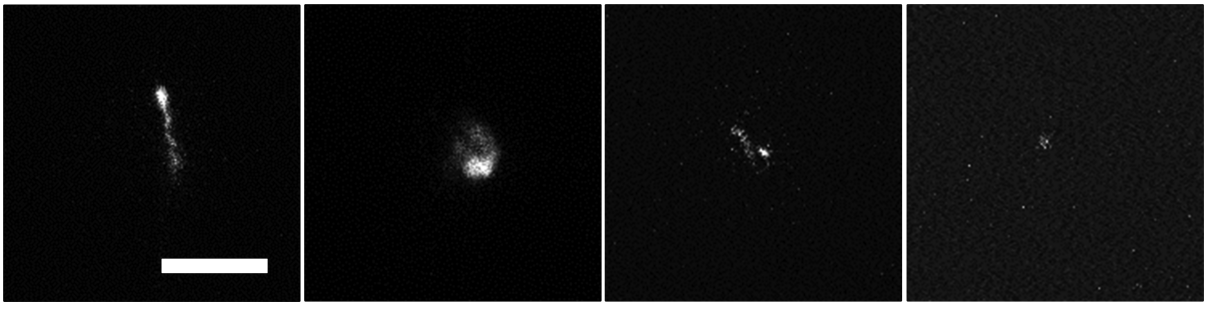

Figure 6. Examples of fracture events; scale bar 1 mm. Swelling in chloroform, imaging at 72.6 Hz (exposure time 12.9 ms). Original 16-bit movie frames are represented in 8 bits for display in this graphic (data analysis performed on 16-bit data).

DOI: 10.1021/acs.macromol.6b02540
Macromolecules 2017, 50, 2043−2053

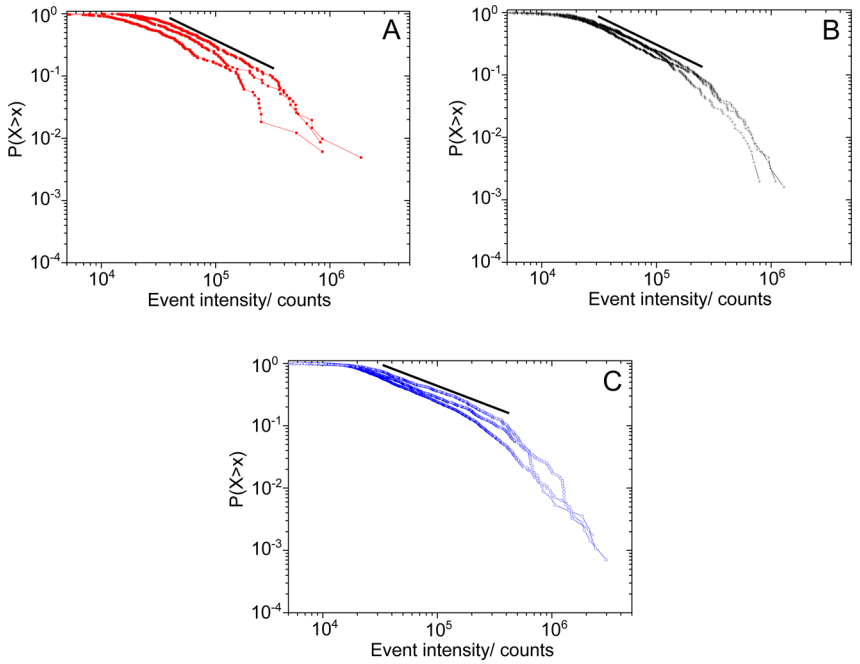

Figure 7. Cumulative distributions of event intensities from highly cross-linked samples, where $P(X > x)$ represents the probability that an event X has an intensity of more than x counts. Total cross-linking density: (A) 4 mol % (red squares); (B) 10 mol % (black crosses); (C) 20 mol % (blue open circles). 0.25 mol % dioxetane cross-linker throughout; tetra(ethylene glycol) inactive cross-linker. Each line represents a separate swelling run. Thick black lines indicate regime in which power law exponents were calculated.

By imaging at a higher frame rate of 503 Hz, we examined in greater detail how single fracture events, such as those shown in Figure 6, propagated through the material. Most gave out light over one to three frames at this frame rate, indicating a typical event duration of 2−6 ms, in agreement with the photodiode measurements at higher sampling rates. Larger events could be observed to advance through the sample over many more frames, as in the example depicted in Figure 8A. This plot shows a single fracture event lasting 75 ms. The centroid of the activated pixels in each frame is represented by a dot that is colored according to the sum of the pixel intensities in that frame. It appears that the tip of the event moves through the material at a rate of approximately 30 mm s^{-1}. Cracks branch off after ∼20 and 60 ms. While the applied stress is not controlled externally in our setup, the observed propagation speed is consistent with rates reported in other swollen gel systems, including a physically cross-linked gelatin hydrogel,[55] a covalently cross-linked polyacrylamide hydrogel,[56] and dual cross-link poly(vinyl alcohol) hydrogels.[57] The spatial extent of the events in each frame is indicated in Figure 8B, which shows the perimeters of the groups of activated pixels over time. The spatial correlation between different rupture events can be further quantified by calculating the probability $C(r)$ that the centroids of two randomly chosen events are separated by a distance smaller than r. This type of analysis is often performed in geology to analyze the spatial relationships between earthquakes or rock fractures.[58] In the case of uncorrelated events, a completely random distribution on the (x, y)-plane is expected, which would give $C(r) \sim r^2$. However, for the events shown in Figure 8A, we find an exponent which is much closer to unity (Figure 8C), which is the value that would be expected for a crack that appears one-dimensional in the (x, y)-plane. We note that the mechanoluminescence most likely originates from a crack plane that extends from the surface through the thickness of the sample (perpendicular to the (x, y)-plane), which appears as one-dimensional in our measurements.

The spatial correlation within the propagating fracture event can be seen by eye from Figure 8A, making the result of Figure 8C rather trivial. However, when investigating the correlation between different fracture events on longer time scales, the spatial relationship between separate events is not readily discerned. Figure 9 shows the mechanoluminescence from 140 separate events recorded during a 3 min time period: the centroids of activated groups of pixels are shown in Figure 9A and the perimeters of the events in Figure 9B. The imaging was performed at a slower frame rate (72.6 Hz) to capture as many events as possible, meaning that each event nearly always appears in just one frame (in contrast to Figure 8). To quantify the correlation between separate events, we calculated the distance and time interval separating every pair of event centroids in the experimental series shown in Figure 9A and then plotted the cumulative probability $C(r)$ in the spatial dimensions (x and y), shown in Figure 9C. A slope of 2 is expected if the fracture events exhibit no spatial clustering; i.e., they are randomly distributed on the (x, y)-plane. A least-squares fit on the distances between *every pair* of events gave a slope of 1.8 over the smallest distances (0.05−0.5 mm, black line); this value progressively decreased to 1.4 for the largest distances (0.5−5 mm). This indicates that the events are almost randomly distributed on the (x, y)-plane with respect to each other, with the number of longer distances limited by the size of the sample (hence leading to a decrease in slope). If only the distances between events that occurred less than 5 s apart are considered (pink line), stronger clustering at the short length scales can be seen, with shorter distances being significantly more likely than longer distances. The spatiotemporal clustering becomes progressively more evident as the time interval between pairs of events is restricted to 0.5 s (blue line) and 0.05 s (green line). Hence, events that are closer in time

DOI: 10.1021/acs.macromol.6b02540
Macromolecules 2017, 50, 2043−2053

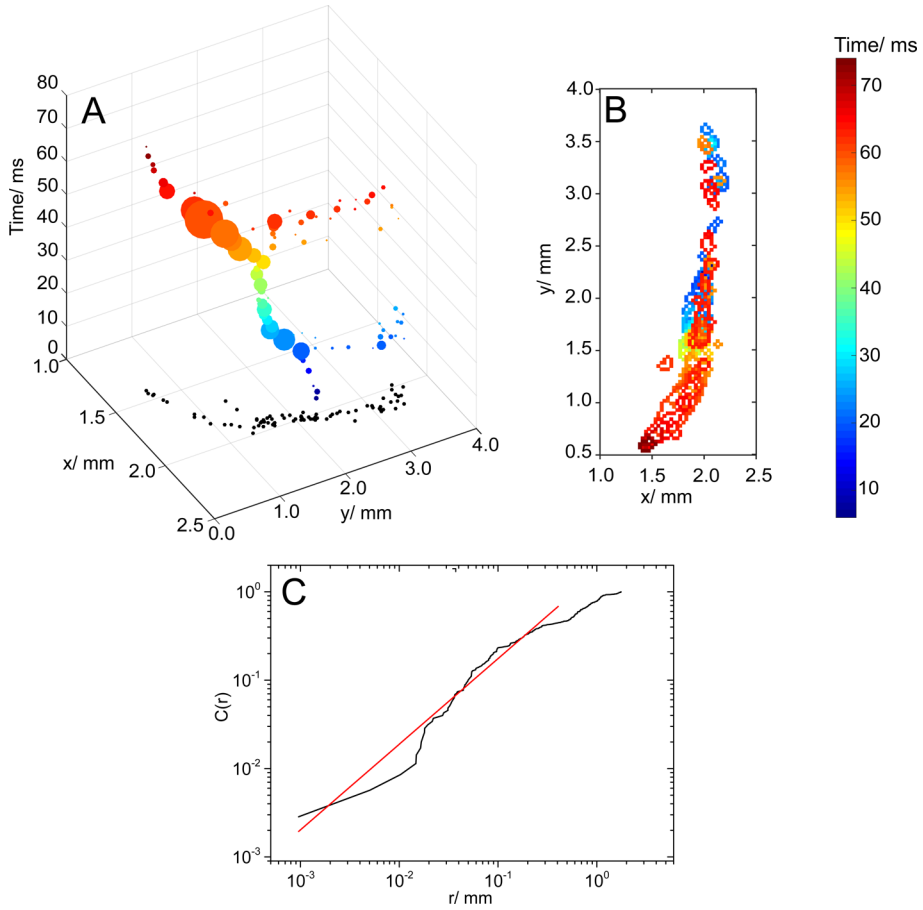

Figure 8. Crack propagation through a sample with 4 mol % total cross-linking density (0.25 mol % dioxetane), fixated with a homemade cell. Imaging at 503.4 Hz (exposure time 1.81 ms). (A) Progression of crack front. Each point represents the centroid of a group of activated pixels with four or more pixels. Each centroid is colored according to time and sized according to the summed intensity of the group of pixels. The projection on the (x, y)-plane is shown in black. (B) Spatial extent of crack with time. The perimeter of every group of activated pixels from (A) is colored according to the time elapsed since crack initiation. (C) The probability $C(r)$ that the distance between a pair of randomly chosen points in (A) has a value less than r. The slope (red line) is fitted by least-squares regression and has a value of 1, as expected for a linear feature. Note that the curve $C(r)$ is quite noisy due to the limited number of data points.

also tend to be closer in space, suggesting that the formation of a crack in the sample promotes the formation of successive cracks in its vicinity, possibly by the creation of new surface area leading to additional solvent sorption.

DISCUSSION

Solvent-induced mechanoluminescence demonstrated unambiguously that osmotic stresses can result in covalent bond scission in cross-linked PMMA. For significant covalent bond scission to occur, it appeared to be necessary both that the matrix is glassy and that the network contains permanent (covalent) cross-links. The solvent front in glassy polymers is much sharper than the typical Fickian concentration profile observed in rubbery networks, as a result of the greater conformational resistance to diffusion posed by the glassy matrix. Covalent bond scission is most likely initiated by the high stresses at the diffusion front, predicted to be of the order of 10 MPa.[19,20] Permanent cross-links may increase the likelihood that the network will deform by covalent bond cleavage, rather than by disruption of interchain interactions, or disentanglement.[9] Earlier work on the swelling of poly(styrene) networks cross-linked with divinylbenzene attributed osmotically induced macroscopic fracture to stresses associated with the sharp diffusion front.[13] There was also a "quiet period" observed at higher cross-linking densities, preceding the main fracture events. This may imply that a certain swelling ratio or degree of plasticization must be reached before covalent bond scission can be initiated: others have suggested that a degree of plasticization, which can be described by a Fickian profile, is necessary before a Case II diffusion front can form in the material.[17,59−61] Higher cross-linking densities may be expected to slow down the initial plasticization, which would lead to a longer induction period. We note however that initiation times can be influenced also by surface effects and sample geometry.

At the diffusion front, the growing swollen part of the network is under compressive stress from the unswollen material, while at the same time exerting a tensile stress on the unswollen phase, favoring crack initiation in the latter. An approximate calibration revealed that 10^9−10^{11} dioxetane bonds undergo scission in each fracture event. For 10^{11} dioxetanes to break, as in the largest single events, a fracture surface of 10−100 mm^2 would need to be created (for estimate, see Supporting Information), which is 1−2 orders of magnitude larger than expected on the basis of the size of our samples and our observations of the swelling process with the camera. The relatively large numbers of bonds involved therefore suggest that the bonds do not only break at the crack tip, but in an extended region around the crack tip. Local plastic deformation

DOI: 10.1021/acs.macromol.6b02540
Macromolecules 2017, 50, 2043−2053

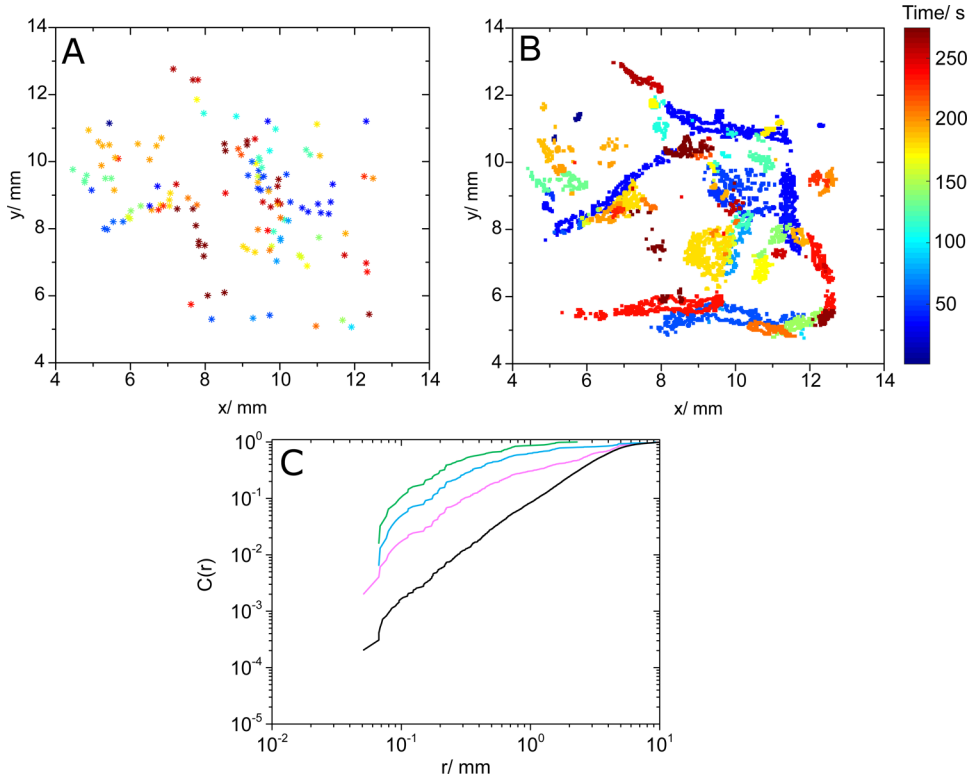

Figure 9. Swelling of sample with 4 mol % total cross-linking density (0.25 mol % dioxetane), fixated in the vial with a homemade cell (for a description of the setup, see Supporting Information). Swelling in chloroform, imaging at 72.6 Hz (exposure time 12.9 ms). (A) Stars represent centroids of 140 events and are colored according to the time elapsed since the beginning of the recording. (B) Perimeters of the same events plotted in a similar way as (A). (C) Probability, $C(r)$, that two events are within a distance r from one another for all events (black line) and for pairs of events that occur less than 5 s apart (pink), 0.5 s apart (blue), and 0.05 s apart (green).

in the glassy phase is most likely to occur via crazing (or cavitation) and the formation of shear zones.[62] Crazes usually nucleate from existing flaws in the material and resemble cracks optically, but in contrast to cracks, crazes remain load-bearing because bundles of polymers, or fibrils, 5−30 nm in diameter, are drawn out of the matrix to span the void between the two craze/bulk interfaces (Figure 10).[63] Forming fibrils requires extensive disentanglement or covalent bond scission, leading to substantial increases (×100) in fracture toughness;[64,65] then, for a craze to become a crack, additional disentanglement or scission must occur to break the fibrils. In simulations, an exponential force distribution was found in the crazes of a glassy polymer, which would favor covalent bond scission.[66] Permanent cross-links make disentanglement more difficult and therefore usually inhibit crazing, but local reductions in T_g as a result of solvent sorption can dramatically lower the stress required for crazing.[67−73] The void channels of existing crazes also provide pathways for the solvent to reach the highly stressed polymer chains at the tip of the craze, and the fibrils themselves, being relatively thin, are readily plasticized, favoring craze (and crack) propagation. A second, competing mode of local plastic deformation in polymer glasses is the orientation of short chain segments to form shear deformation zones, which proceeds without the creation of voids and therefore does not necessarily require the breakdown of entanglements or bond scission.[74] The competition between shear deformation and crazing is strongly dependent on the polymer glass and the experimental conditions.[75,76] A study of the sorption of Freon 113 ($Cl_2FCCClF_2$) by polystyrene networks found that solvent diffusion led to the creation of both shear deformation zones

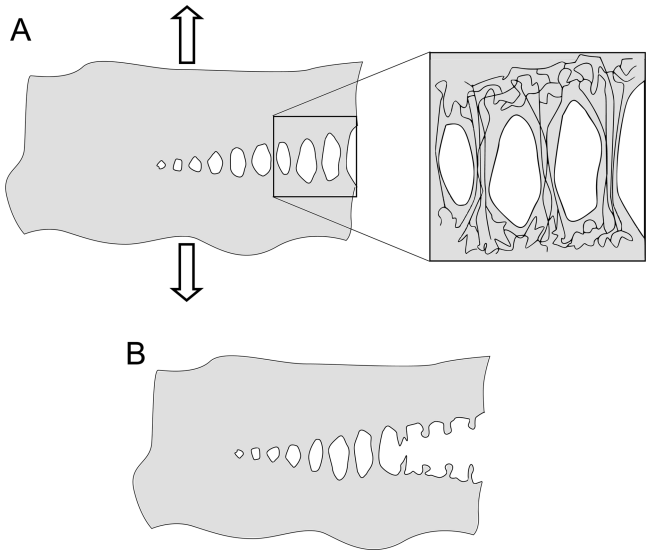

Figure 10. Schematic showing (A) the structure of a craze formed under tensile stress, with aligned polymer chains within the fibrils and microvoids between the fibrils, and (B) the propagation of a crack by fibril breakdown.

and crazes, with shear deformation favored at higher cross-linking densities.[62] The intensity of the mechanoluminescence from our system shows that it is likely that crazing or cavitation forms at least a part of the response of PMMA to osmotic stress, as confirmed by the observation of whitening in the

DOI: 10.1021/acs.macromol.6b02540
Macromolecules 2017, 50, 2043−2053

sample following swelling (see Supporting Information), and increasingly so at higher cross-linking densities.

In the highly cross-linked samples, hundreds of mechanoluminescent fracture events could be observed, apparently randomly distributed in time and intensity. The numbers of bonds involved in the individual fracture events could not be described by a normal distribution, but instead spanned 2 orders of magnitude, with a high degree of skew in the distribution toward rupture events involving smaller numbers of bonds. Similar behavior has been reported in the fracture of other brittle media, which in some cases was characterized as a power law distribution[77,78,78,79] and in others as log-normals or stretched exponentials.[80,81] Fitting a power law to the cumulative distribution of intensities, an exponent of 0.83 is obtained over at least 1 decade of intensity, which is similar to the value of 0.8 found for classic stick−slip behavior in, for example, the distribution of earthquake magnitudes.[82] A power-law relationship can be an expression of scale-free behavior, i.e., that the fracture events can involve any number of bonds, subject to cutoffs defined by the physical limits of the system under study. In our data, there is an upper cutoff (corresponding to an event area of approximately 0.3 mm^2), defined by the dimensions of the sample being swollen, and a lower cutoff, which originates from the resolution of the image, since a weak signal in a single pixel cannot be distinguished from shot noise with similar intensity. A diverse range of physical interpretations have been proposed for power-law behavior, but the concept of self-organized criticality (SOC) is perhaps the most relevant to our system, which has been invoked or referenced in previous studies on fracture processes.[83,84] SOC describes the ability of some dynamic systems on slow driving to progress spontaneously toward a critical state, regardless of their starting state; perturbations lead to sudden avalanches (as opposed to gradual changes), the magnitudes of which follow a power-law distribution. Here, slow driving from the moving solvent front leads to avalanches of bond-breaking. Nevertheless, log-normal and stretched exponential distributions could also describe the observed skew toward smaller events. These distributions express mechanisms in which the effects of independent variables are multiplicative, such as the existing distribution of defects and the distribution of stresses at the solvent front. The relatively narrow intensity range of the data makes it difficult to distinguish between these outwardly similar distributions.

Lastly, camera imaging furnished direct spatial information about the size and length of the fracture events and their position. For example, clustering at short time and length scales, most likely resulting from crack or craze propagation, could be seen. We were also able to estimate fracture propagation rates with this technique, which were found to be relatively slow for glassy materials. Crack propagation in PMMA has been reported to proceed at velocities ranging from 10^{-10} to 100 m s^{-1},[63] depending on the local stresses at the crack tips, as described by the stress intensity factor, K_I. The relatively slow propagation rate would suggest that the cracks experience a stress intensity factor that is less than the critical value required for fast propagation, K_{IC}.

CONCLUSIONS

Mechanoluminescence demonstrated that osmotic pressure applied to a glassy polymer network led to localized cascades of covalent bond-breaking, which were probably initiated at a sharp, relaxation-controlled diffusion front. While it can be seen by eye that some long (∼1 mm) cracks formed at higher cross-linking densities, mechanoluminescence revealed that a smaller but significant proportion of bonds involved in fracture were in fact broken in smaller bond-breaking events, with most lasting a few milliseconds. A calibration allowed us to estimate that each event involved the scission of 10^9−10^{11} dioxetane moieties, suggesting that crack formation initiated in the glassy, unswollen part of the network, but with significant localized yielding, such as crazing. The bursts of bond-breaking observed in our experiments most likely result from the failure of plasticized fibrils within the crazes. Furthermore, spatial analysis indicated some spatiotemporal clustering of fractures and, at higher frame rates, crack/craze propagation within individual fracture events. In comparison with existing techniques to monitor covalent bond scission in glassy polymers, such as acoustic emission,[56] mechanoluminescence offers exciting advantages highlighted by this work, including direct visualization, temporal resolution, and molecular-level quantification. We envisage that mechanoluminescence could be fruitfully employed to study localized fracture events in polymers in a wide range of loading scenarios.

ASSOCIATED CONTENT

Supporting Information

The Supporting Information is available free of charge on the ACS Publications website at DOI: 10.1021/acs.macromol.6b02540.

Figures S1−S4 (PDF)

AUTHOR INFORMATION

Corresponding Author

*E-mail: r.p.sijbesma@tue.nl (R.P.S.).

ORCID

Rint P. Sijbesma: 0000-0002-8975-636X

Funding

This work has been financially supported by the Council for Chemical Sciences of The Netherlands Organization for Scientific Research (CW-NOW grant 726.011.002) and by the Ministry of Education, Culture and Science of The Netherlands (Gravity program 024.001.035). J.v.d.G. acknowledges support from the European Research Council (ERC Consolidator Grant "Softbreak").

Notes

The authors declare no competing financial interest.

ACKNOWLEDGMENTS

A group of Master's students contributed to the initial development of this project: Jiangmiao Yuan, Sisi Tang, Tom Heijmans, Yong Niu, and He Wu. We thank Prof. Thijs Michels and Prof. Costantino Creton for helpful discussions.

REFERENCES

(1) International, A. S. M.; Lampman, S. *Characterization and Failure Analysis of Plastics*; ASM International: 2003.

(2) van Westing, E. P. M.; Ferrari, G. M.; de Wit, J. H. W. The Determination of Coating Performance with Impedance measurements—II. Water Uptake of Coatings. *Corros. Sci.* **1994**, *36* (6), 957−977.

(3) Bolto, B.; Tran, T.; Hoang, M.; Xie, Z. Crosslinked Poly(vinyl Alcohol) Membranes. *Prog. Polym. Sci.* **2009**, *34* (9), 969−981.

DOI: 10.1021/acs.macromol.6b02540
Macromolecules 2017, 50, 2043−2053

(4) Gebel, G. Structural Evolution of Water Swollen Perfluorosulfonated Ionomers from Dry Membrane to Solution. *Polymer* **2000**, *41* (15), 5829−5838.
(5) Hodge, R. M.; Edward, G. H.; Simon, G. P. Water Absorption and States of Water in Semicrystalline Poly(vinyl Alcohol) Films. *Polymer* **1996**, *37* (8), 1371−1376.
(6) Peppas, N. A.; Hilt, J. Z.; Khademhosseini, A.; Langer, R. Hydrogels in Biology and Medicine: From Molecular Principles to Bionanotechnology. *Adv. Mater.* **2006**, *18* (11), 1345−1360.
(7) Korsmeyer, R. W.; Gurny, R.; Doelker, E.; Buri, P.; Peppas, N. A. Mechanisms of Solute Release from Porous Hydrophilic Polymers. *Int. J. Pharm.* **1983**, *15* (1), 25−35.
(8) Bell, C. L.; Peppas, N. A. An Apparatus to Measure Polymer Swelling under Load. *Int. J. Pharm.* **1996**, *134* (1), 167−172.
(9) Miller-Chou, B. A.; Koenig, J. L. A Review of Polymer Dissolution. *Prog. Polym. Sci.* **2003**, *28* (8), 1223−1270.
(10) Gourianova, S.; Fuhrmann, J. Depth Profiling of Ultrathin P(S-B-MMA) Diblock Copolymer Films by Selective Solvent Crazing. *Macromolecules* **2004**, *37* (5), 1825−1830.
(11) Rahmanian, O.; Chen, C.-F.; DeVoe, D. L. Microscale Patterning of Thermoplastic Polymer Surfaces by Selective Solvent Swelling. *Langmuir* **2012**, *28* (35), 12923−12929.
(12) Zavala-Rivera, P.; Channon, K.; Nguyen, V.; Sivaniah, E.; Kabra, D.; Friend, R. H.; Nataraj, S. K.; Al-Muhtaseb, S. A.; Hexemer, A.; Calvo, M. E.; Miguez, H. Collective Osmotic Shock in Ordered Materials. *Nat. Mater.* **2011**, *11* (1), 53−57.
(13) Alfrey, T.; Gurnee, E. F.; Lloyd, W. G. Diffusion in Glassy Polymers. *J. Polym. Sci., Part C: Polym. Symp.* **1966**, *12* (1), 249−261.
(14) Robeson, L. M. Environmental Stress Cracking: A Review. *Polym. Eng. Sci.* **2013**, *53* (3), 453−467.
(15) Kefalas, V. A. Solvent Crazing as a Stress-Induced Surface Adsorption and Bulk Plasticization Effect. *J. Appl. Polym. Sci.* **1995**, *58* (4), 711−717.
(16) Thomas, N. L.; Windle, A. H. A Deformation Model for Case II Diffusion. *Polymer* **1980**, *21* (6), 613−619.
(17) Hui, C.-Y.; Wu, K.-C.; Lasky, R. C.; Kramer, E. J. Case-II Diffusion in Polymers. I. Transient Swelling. *J. Appl. Phys.* **1987**, *61* (11), 5129−5136.
(18) Hui, C.-Y.; Wu, K.-C.; Lasky, R. C.; Kramer, E. J. Case-II Diffusion in Polymers. II. Steady-state Front Motion. *J. Appl. Phys.* **1987**, *61* (11), 5137−5149.
(19) Thomas, N. L.; Windle, A. H. A Theory of Case II Diffusion. *Polymer* **1982**, *23* (4), 529−542.
(20) Sarti, G. C. Solvent Osmotic Stresses and the Prediction of Case II Transport Kinetics. *Polymer* **1979**, *20* (7), 827−832.
(21) Bhattacharya, S.; Sharma, D. K.; Saurabh, S.; De, S.; Sain, A.; Nandi, A.; Chowdhury, A. Plasticization of Poly(vinylpyrrolidone) Thin Films under Ambient Humidity: Insight from Single-Molecule Tracer Diffusion Dynamics. *J. Phys. Chem. B* **2013**, *117* (25), 7771−7782.
(22) Gall, T. P.; Lasky, R. C.; Kramer, E. J. Case II Diffusion: Effect of Solvent Molecule Size. *Polymer* **1990**, *31* (8), 1491−1499.
(23) Ercken, M.; Adriaensens, P.; Vanderzande, D.; Gelan, J. Study of Solvent Diffusion in Polymeric Materials Using Magnetic Resonance Imaging. *Macromolecules* **1995**, *28* (25), 8541−8547.
(24) McGarel, O. J.; Wool, R. P. Craze Growth and Healing in Polystyrene. *J. Polym. Sci., Part B: Polym. Phys.* **1987**, *25* (12), 2541−2560.
(25) Stamatialis, D. F.; Sanopoulou, M.; Petropoulos, J. H. Investigation of Case II Diffusion Behavior. 2. Study of the Poly(methyl methacrylate)−Methyl Alcohol System by Two-Beam Microinterferometry. *Macromolecules* **2002**, *35* (3), 1021−1027.
(26) Bagrov, D. v.; Yarysheva, A. y.; Rukhlya, E. g.; Yarysheva, L. m.; Volynskii, A. l.; Bakeev, N. f. Atomic Force Microscopic Study of the Structure of High-Density Polyethylene Deformed in Liquid Medium by Crazing Mechanism. *J. Microsc.* **2014**, *253* (2), 151−160.
(27) Shibayama, M. Small-Angle Neutron Scattering on Polymer Gels: Phase Behavior, Inhomogeneities and Deformation Mechanisms. *Polym. J.* **2011**, *43* (1), 18−34.
(28) Cornélis, H.; Kander, R. G. A New Method to Evaluate Solvent Stress Cracking. *Polym. Eng. Sci.* **1996**, *36* (6), 869−878.
(29) Arifuzzaman, M.; Wu, Z. L.; Takahashi, R.; Kurokawa, T.; Nakajima, T.; Gong, J. P. Geometric and Edge Effects on Swelling-Induced Ordered Structure Formation in Polyelectrolyte Hydrogels. *Macromolecules* **2013**, *46* (22), 9083−9090.
(30) Davis, D. A.; Hamilton, A.; Yang, J.; Cremar, L. D.; Van Gough, D.; Potisek, S. L.; Ong, M. T.; Braun, P. V.; Martínez, T. J.; White, S. R.; Moore, J. S.; Sottos, N. R. Force-Induced Activation of Covalent Bonds in Mechanoresponsive Polymeric Materials. *Nature* **2009**, *459* (7243), 68−72.
(31) Chen, Y.; Spiering, A. J. H.; Karthikeyan, S.; Peters, G. W. M.; Meijer, E. W.; Sijbesma, R. P. Mechanically Induced Chemiluminescence from Polymers Incorporating a 1,2-Dioxetane Unit in the Main Chain. *Nat. Chem.* **2012**, *4* (7), 559−562.
(32) Ramirez, A. L. B.; Kean, Z. S.; Orlicki, J. A.; Champhekar, M.; Elsakr, S. M.; Krause, W. E.; Craig, S. L. Mechanochemical Strengthening of a Synthetic Polymer in Response to Typically Destructive Shear Forces. *Nat. Chem.* **2013**, *5* (9), 757−761.
(33) Kean, Z. S.; Niu, Z.; Hewage, G. B.; Rheingold, A. L.; Craig, S. L. Stress-Responsive Polymers Containing Cyclobutane Core Mechanophores: Reactivity and Mechanistic Insights. *J. Am. Chem. Soc.* **2013**, *135* (36), 13598−13604.
(34) Piermattei, A.; Karthikeyan, S.; Sijbesma, R. P. Activating Catalysts with Mechanical Force. *Nat. Chem.* **2009**, *1* (2), 133−137.
(35) Groote, R.; Szyja, B. M.; Pidko, E. A.; Hensen, E. J. M.; Sijbesma, R. P. Unfolding and Mechanochemical Scission of Supramolecular Polymers Containing a Metal−Ligand Coordination Bond. *Macromolecules* **2011**, *44* (23), 9187−9195.
(36) Jakobs, R. T. M.; Ma, S.; Sijbesma, R. P. Mechanocatalytic Polymerization and Cross-Linking in a Polymeric Matrix. *ACS Macro Lett.* **2013**, *2* (7), 613−616.
(37) Plunkett, K. N.; Kraft, M. L.; Yu, Q.; Moore, J. S. Swelling Kinetics of Disulfide Cross-Linked Microgels. *Macromolecules* **2003**, *36* (11), 3960−3966.
(38) Hickenboth, C. R.; Rule, J. D.; Moore, J. S. Preparation of Enediyne-Crosslinked Networks and Their Reactivity under Thermal and Mechanical Conditions. *Tetrahedron* **2008**, *64* (36), 8435−8448.
(39) Lee, C. K.; Diesendruck, C. E.; Lu, E.; Pickett, A. N.; May, P. A.; Moore, J. S.; Braun, P. V. Solvent Swelling Activation of a Mechanophore in a Polymer Network. *Macromolecules* **2014**, *47* (8), 2690−2694.
(40) Lyu, B.; Cha, W.; Mao, T.; Wu, Y.; Qian, H.; Zhou, Y.; Chen, X.; Zhang, S.; Liu, L.; Yang, G.; Lu, Z.; Zhu, Q.; Ma, H. Surface Confined Retro Diels−Alder Reaction Driven by the Swelling of Weak Polyelectrolytes. *ACS Appl. Mater. Interfaces* **2015**, *7* (11), 6254−6259.
(41) Clough, J. M.; Sijbesma, R. P. Dioxetane Scission Products Unchanged by Mechanical Force. *ChemPhysChem* **2014**, *15* (16), 3565−3571.
(42) Chen, Y.; Sijbesma, R. P. Dioxetanes as Mechanoluminescent Probes in Thermoplastic Elastomers. *Macromolecules* **2014**, *47* (12), 3797−3805.
(43) Ducrot, E.; Chen, Y.; Bulters, M.; Sijbesma, R. P.; Creton, C. Toughening Elastomers with Sacrificial Bonds and Watching Them Break. *Science* **2014**, *344* (6180), 186−189.
(44) Kean, Z. S.; Hawk, J. L.; Lin, S.; Zhao, X.; Sijbesma, R. P.; Craig, S. L. Increasing the Maximum Achievable Strain of a Covalent Polymer Gel Through the Addition of Mechanically Invisible Cross-Links. *Adv. Mater.* **2014**, *26* (34), 6013−6018.
(45) Clough, J. M.; Creton, C.; Craig, S. L.; Sijbesma, R. P. Covalent Bond Scission in the Mullins Effect of a Filled Elastomer: Real-Time Visualization with Mechanoluminescence. *Adv. Funct. Mater.* **2016**, *26*, 9063.
(46) Wieringa, J. H.; Strating, J.; Wynberg, H.; Adam, W. Adamantylideneadamantane Peroxide, a Stable 1,2-Dioxetane. *Tetrahedron Lett.* **1972**, *13* (2), 169−172.
(47) Hummelen, J. C.; Luider, T. M.; Wynberg, H. Functionalized Adamantylideneadamantane 1,2-Dioxetanes: Investigations on Stable

DOI: 10.1021/acs.macromol.6b02540
Macromolecules 2017, 50, 2043−2053

and Inherently Chemiluminescent Compounds as a Tool for Clinical Analysis. *Pure Appl. Chem.* **1987**, *59* (5), 639−650.
(48) Meijer, E. W.; Wynberg, H. The Synthesis and Chemiluminescence of Stable 1,2-Dioxetane: An Organic Chemistry Laboratory Experiment. *J. Chem. Educ.* **1982**, *59* (12), 1071.
(49) Birch, D. J. S.; Imhof, R. E. Fluorescence Lifetimes and Relative Quantum Yields of 9,10-Diphenylanthracene in Dilute Solutions of Cyclohexane and Benzene. *Chem. Phys. Lett.* **1975**, *32* (1), 56−58.
(50) Charney, D. R.; Dalton, J. C.; Hautala, R. R.; Snyder, J. J.; Turro, N. J. Evidence for Comparable Reactivity of Alkanone Excited Singlet and Triplet States toward Hydrogen Donors. *J. Am. Chem. Soc.* **1974**, *96* (5), 1407−1410.
(51) Turro, N. J.; Kochevar, I. E.; Noguchi, Y.; Chow, M.-F. Electronic Excitation Transfer in Polymers. 3. Singlet-Singlet, Triplet-Singlet, and Triplet-Triplet Energy Transfers. Evidence for Triplet Migration among Pendant Phenyl Groups of Polystyrene. *J. Am. Chem. Soc.* **1978**, *100* (10), 3170−3177.
(52) Wiley-VCH. *Ullmann's Polymers and Plastics, 4 Vol. Set: Products and Processes*; John Wiley & Sons: 2016.
(53) Williams, D. R. G.; Allen, P. E. M.; Truong, V. T. Glass Transition Temperature and Stress Relaxation of Methanol Equilibrated Poly(methyl Methacrylate). *Eur. Polym. J.* **1986**, *22* (11), 911−919.
(54) Lin, C. B.; Liu, K. S.; Lee, S. Methanol-Induced Opacity in Poly (Methyl Methacrylate). *J. Polym. Sci., Part B: Polym. Phys.* **1991**, *29* (12), 1457−1466.
(55) Baumberger, T.; Caroli, C.; Martina, D. Solvent Control of Crack Dynamics in a Reversible Hydrogel. *Nat. Mater.* **2006**, *5* (7), 552−555.
(56) Livne, A.; Cohen, G.; Fineberg, J. Universality and Hysteretic Dynamics in Rapid Fracture. *Phys. Rev. Lett.* **2005**, *94* (22), 224301.
(57) Mayumi, K.; Guo, J.; Narita, T.; Hui, C. Y.; Creton, C. Fracture of Dual Crosslink Gels with Permanent and Transient Crosslinks. *Extreme Mech. Lett.* **2016**, *6*, 52−59.
(58) Tosi, P.; De Rubeis, V.; Loreto, V.; Pietronero, L. Space−time Correlation of Earthquakes. *Geophys. J. Int.* **2008**, *173* (3), 932−941.
(59) Ekenseair, A. K.; Peppas, N. A. Network Structure and Methanol Transport Dynamics in Poly(methyl Methacrylate). *AIChE J.* **2012**, *58* (5), 1600−1609.
(60) Hassan, M. M.; Durning, C. J. Effects of Polymer Molecular Weight and Temperature on Case II Transport. *J. Polym. Sci., Part B: Polym. Phys.* **1999**, *37* (22), 3159−3171.
(61) Lasky, R. C.; Kramer, E. J.; Hui, C.-Y. The Initial Stages of Case II Diffusion at Low Penetrant Activities. *Polymer* **1988**, *29* (4), 673−679.
(62) Miller, P.; Kramer, E. J. Environmental Shear Deformation Zones and Crazes in Crosslinked Polystyrene and Poly(para-Methylstyrene). *J. Mater. Sci.* **1990**, *25* (3), 1751−1761.
(63) Döll, W. Optical Interference Measurements and Fracture Mechanics Analysis of Crack Tip Craze Zones. In *Crazing in Polymers*; Kausch, H. H., Ed.; Advances in Polymer Science; Springer: Berlin, 1983; pp 105−168.
(64) Henkee, C. S.; Kramer, E. J. Loss of Entanglement Density during Crazing. *J. Mater. Sci.* **1986**, *21* (4), 1398−1404.
(65) Donald, A. M.; Kramer, E. J. Effect of Molecular Entanglements on Craze Microstructure in Glassy Polymers. *J. Polym. Sci., Polym. Phys. Ed.* **1982**, *20* (5), 899−909.
(66) Rottler, J.; Robbins, M. O. Growth, Microstructure, and Failure of Crazes in Glassy Polymers. *Phys. Rev. E* **2003**, *68* (1), 11801.
(67) Graham, I. D.; Williams, J. G.; Zichy, E. L. Craze Kinetics for PMMA in Liquids. *Polymer* **1976**, *17* (5), 439−442.
(68) Andrews, E. H.; Levy, G. M. Solvent Stress Crazing in PMMA: 1. Geometrical Effects. *Polymer* **1974**, *15* (9), 599−607.
(69) Kambour, R. P.; Gruner, C. L.; Romagosa, E. E. Solvent Crazing of "dry" Polystyrene and "dry" Crazing of Plasticized Polystyrene. *J. Polym. Sci., Polym. Phys. Ed.* **1973**, *11* (10), 1879−1890.
(70) Kambour, R. P.; Gruner, C. L.; Romagosa, E. E. Biphenol-A Polycarbonate Immersed in Organic Media. Swelling and Response to Stress. *Macromolecules* **1974**, *7* (2), 248−253.
(71) Kambour, R. P.; Chu, C.; Avakian, R. W. Crystallizing Crazes: The Probable Source of Solvent Stress Cracking Resistance in a Polyester/Polycarbonate Blend. *J. Polym. Sci., Part B: Polym. Phys.* **1986**, *24* (9), 2135−2144.
(72) Mai, Y.-W. Environmental Stress Cracking of Glassy Polymers and Solubility Parameters. *J. Mater. Sci.* **1986**, *21* (3), 904−916.
(73) Bigg, D. M.; Leininger, R. I.; Lee, C. S. Stress Cracking Behaviour of Poly(methyl Methacrylate) and a Poly(methyl Methacrylate-Ethyl Acrylate) Copolymer. *Polymer* **1981**, *22* (4), 539−542.
(74) Deblieck, R. A. C.; van Beek, D. J. M.; Remerie, K.; Ward, I. M. Failure Mechanisms in Polyolefines: The Role of Crazing, Shear Yielding and the Entanglement Network. *Polymer* **2011**, *52* (14), 2979−2990.
(75) Kramer, E. J.; Berger, L. L. Fundamental Processes of Craze Growth and Fracture. In *Crazing in Polymers*; Kausch, H.-H., Ed.; Advances in Polymer Science; Springer: Berlin, 1990; Vol. 2, pp 1−68.
(76) Donald, A. M.; Kramer, E. J. The Competition between Shear Deformation and Crazing in Glassy Polymers. *J. Mater. Sci.* **1982**, *17* (7), 1871−1879.
(77) Maes, C.; Van Moffaert, A.; Frederix, H.; Strauven, H. Criticality in Creep Experiments on Cellular Glass. *Phys. Rev. B: Condens. Matter Mater. Phys.* **1998**, *57* (9), 4987−4990.
(78) Garcimartín, A.; Guarino, A.; Bellon, L.; Ciliberto, S. Statistical Properties of Fracture Precursors. *Phys. Rev. Lett.* **1997**, *79* (17), 3202−3205.
(79) Mäkinen, T.; Miksic, A.; Ovaska, M.; Alava, M. J. Avalanches in Wood Compression. *Phys. Rev. Lett.* **2015**, *115* (5), 55501.
(80) Clauset, A.; Shalizi, C. R.; Newman, M. E. J. Power-Law Distributions in Empirical Data. *SIAM Rev.* **2009**, *51* (4), 661−703.
(81) Newman, M. E. J. Power Laws, Pareto Distributions and Zipf's Law. *Contemp. Phys.* **2005**, *46* (5), 323−351.
(82) Bak, P.; Christensen, K.; Danon, L.; Scanlon, T. Unified Scaling Law for Earthquakes. *Phys. Rev. Lett.* **2002**, *88* (17), 178501.
(83) Sprakel, J.; Spruijt, E.; Stuart, M. A. C.; Michels, M. A. J.; van der Gucht, J. Intermittent Dynamics in Transient Polymer Networks under Shear: Signs of Self-Organized Criticality. *Phys. Rev. E* **2009**, *79* (5), 56306.
(84) Zapperi, S.; Vespignani, A.; Stanley, H. E. Plasticity and Avalanche Behaviour in Microfracturing Phenomena. *Nature* **1997**, *388* (6643), 658−660.

DOI: 10.1021/acs.macromol.6b02540
Macromolecules 2017, 50, 2043−2053